# Theoretical Studies on Solvent and Substituent Effects of Cuprate Conjugate Addition

Masahiro Yamanaka and Eiichi Nakamura*

*Department of Chemistry, The University of Tokyo, Tokyo 113-0033, Japan*

*Received June 18, 2001*

Conjugate addition of lithium diorganocuprate to acrolein, cyclohexenone, and 4,4-dimethylcyclohexenone has been studied in the presence of $Me_2O$ molecules coordinated on the lithium atoms. Solvation does not change the mechanism of the conjugate addition but increases the activation energy of the C−C bond-forming step through attenuation of the Lewis acidity of the lithium atoms. The substituent on the enone electrophile was found to have considerable influence on the activation energy. Computed activation energy of the conjugate addition of lithium dimethylcuprate to 4,4-dimethylcyclohexenone is $\Delta E^{\ddagger} = 15.5$ kcal/mol, which is close to the experimental data ($E_a = 18.2 \pm 1.7$ kcal/mol). The $^{12}C/^{13}C$ kinetic isotope effects were found to be susceptible to substituent effects. The $^{13}C$ NMR chemical shift values qualitatively agree with experimental data.



Conjugate addition reactions of organocuprates to α,β-unsaturated carbonyl compounds have long been a subject of interest to chemists, but the mechanism has remained unclear for a long time. We previously approached the mechanistic issues with ab initio and the density functional calculations (B3LYP/631AS)[1] and studied the conjugate addition of $(Me_2CuLi)_2$ to acrolein[2b] and cyclohexenone[2c] to find that the reductive C−C bond-forming step (i.e., **TS**) via the Cu(III) intermediate (i.e., **CP**) is the crucial step of the reaction[3] (Scheme 1).

In previous studies,[2,4] simple model species (i.e., $(Me_2CuLi)_2$ + acrolein or cyclohexenone) without solvent coordination were generally employed due to computational limitation at the time of studies. As shown by $^1H$, $^6Li$ HOESY NMR investigations[5] of organocuprates in solution, the structure and reactivity of organocuprates strongly depend on the solvent coordination of the Lewis acidic lithium atoms. The contact ion pair (CIP) (e.g. **RT** in Scheme 1) is predominantly formed in $Et_2O$. On the other hand, the separated ion pair (SSIP) is thermodynamically favored in THF or in the presence of crown ether or HMPA. The correlation of the reactivity to the structural change is an important issue. Krause recently reported the first data of the activation energies of cuprate conjugate addition reactions,[6] and it has become possible to compare the experimental and theoretical activation energies. In the reaction between 4,4-dimethylcyclohexenone and $Me_2CuLi{\cdot}LiI$, the activation energy has been measured to be $E_a = 18.2 \pm 1.7$ kcal/mol. This value is much larger than the computational value we obtained for cyclohexenone and $Me_2CuLi{\cdot}LiCl$ without solvent coordination[2c] ($\Delta E^{\ddagger} = 10.9$ kcal/mol at the B3LYP/631AS level) and cast some doubt on the accuracy of our computational results. We herein report the results of the studies on the solvent and the substituent effects of cuprate conjugate addition, which gave us an activation energy of $\Delta E^{\ddagger} = 15.5$ kcal/mol—a value quite close to the experimental data.

**Scheme 1**

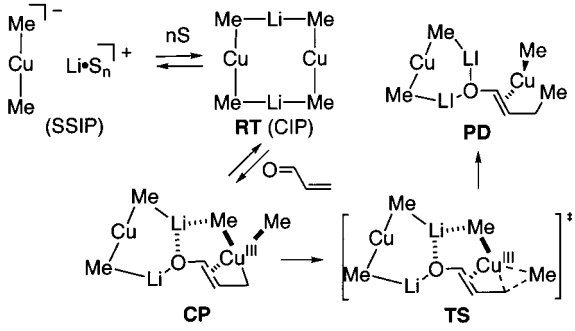


* To whom correspondence should be addressed. E-mail: nakamura@chem.s.u-tokyo.ac.jp.

(1) (a) For pertinent references on cuprate mechanisms, see: Nakamura, E.; Mori, S. *Angew. Chem., Int. Ed.* **2000**, *39*, 3751−3771. (b) Lipshutz, B. H.; Sengupta, S. *Org. React.* **1992**, *41*, 135−631. (c) Krause, N.; Gerold, A. *Angew. Chem., Int. Ed. Engl.* **1997**, *36*, 186−204.

(2) (a) Nakamura, E.; Mori, S.; Nakamura, M.; Morokuma, K. *J. Am. Chem. Soc.* **1997**, *119*, 4887−4899. (b) Nakamura, E.; Mori, S.; Morokuma, K. *J. Am. Chem. Soc.* **1997**, *119*, 4900−4910. (c) Mori, S.; Nakamura, E. *Chem. Eur. J.* **1999**, 5, 1534−1543. (d) Nakamura, E.; Yamanaka, M. *J. Am. Chem. Soc.* **1999**, *121*, 8941−8942.

(3) Krauss, S. R.; Smith, S. G. *J. Am. Chem. Soc.* **1981**, *103*, 141−148.

(4) (a) Nakamura, E.; Mori, S.; Morokuma, K. *J. Am. Chem. Soc.* **1998**, *120*, 8273−8274. (b) Mori, S.; Nakamura, E. *Chem. Eur. J.* **1999**, *5*, 1534−1543. (c) Mori, S.; Nakamura, E. *J. Mol. Struct. (THEOCHEM)* **1999**, *461−462*, 167−175. (d) Mori, S.; Nakamura, E. *Tetrahedron Lett.* **1999**, *40*, 5319−5322. (e) Mori, S.; Nakamura, E.; Morokuma, K. *J. Am. Chem. Soc.* **2000**, *122*, 7294−7307. (f) Mori, S.; Hirai, A.; Nakamura, M.; Nakamura, E. *Tetrahedron* **2000**, *56*, 2805−2809. (g) Nakamura, E.; Yamanaka, M.; Yoshikai, N.; Mori, S. *Angew. Chem., Int. Ed.* **2001**, *40*, 1935−1938.

(5) (a) Gschwind, R. M.; Rajamohanan, P. R.; John, M.; Boche, G. *Organometallics* **2000**, *19*, 2868−2873. (b) John, M.; Auel, C.; Behrens, C.; Marsch, M.; Harms, K.; Bosold, F.; Gschwind, R. M.; Rajamohanan, P. R.; Boche, G. *Chem. Eur. J.* **2000**, *6*, 3060−3068. (c) Gschwind, R. M.; Pattuparambil, X. X.; Rajamohanan, P. R.; Auel, C.; Boche, G. *J. Am. Chem. Soc.* **2001**, *123*, 7299−7304.

(6) Canisius, J.; Gerold, A.; Krause, N. *Angew. Chem., Int. Ed.* **1999**, *38*, 1644−1646.

10.1021/om0105270 CCC: $20.00 
Publication on Web 11/22/2001

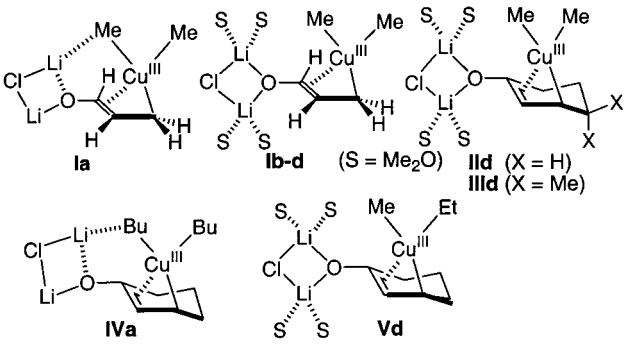


**Figure 1.** Chemical models.

## Chemical Models

Since the cuprate reactions are normally carried out in ether and THF,[1,7] we employed dimethyl ether as a model solvent. We started from nonsolvated model (**Ia**) that we reported previously and added an increasing number of $Me_2O$ molecules until four-coordination of the lithium atoms is achieved (series of **b**−**d**: **b**, $2Me_2O$; **c**, $3Me_2O$; **d**, $4Me_2O$). Since the copper atoms in these models are coordinatively saturated (organocuprate(I) species, dicoordinated; organocuprate(III) species, tetracoordinated),[1d] only the solvent coordination on the lithium atoms was examined. The electronic and geometric properties of the solvated models in the reaction of $Me_2CuLi{\cdot}LiCl$ and acrolein (**Ib**−**d**) were first examined to probe the issue of solvent effects (Figure 1).

To examine the effects of the substituents on the reactant, the reactions of $Me_2CuLi{\cdot}LiCl$ with cyclohexenone (i.e., **IId**) and 4,4-dimethylcyclohexenone (i.e., **IIId**) were studied.[6] The nonsolvated model **IVa**, $Bu_2CuLi{\cdot}LiCl$, reacting with cyclohexenone and the corresponding solvated model **IId** were examined to study the solvent and substituent effects on the $^{12/13}C$ kinetic isotope effects (KIEs). In addition, the solvated model of the reaction of Me(Et)CuLi·LiCl and cyclohexenone (**Vd**) was also studied to make a comparison with the solvated $Me_2CuLi{\cdot}LiCl$ and the nonsolvated $Bu_2CuLi{\cdot}LiCl$. The solvent coordination effect on the $^{13}C$ NMR chemical shift was examined for the solvated model of $Me_2CuLi{\cdot}LiCl$ and cyclohexenone (**IId**).

## Computational Methods

All calculations were performed with the GAUSSIAN 98 package.[8] Geometry optimization was performed at the B3LYP level with the basis set denoted as 321AS and 631AS consisting of Ahlrichs-SVP all-electron basis set[9] for the Cu atom and 3-21G[10] and 6-31G(d)[10] for the rest.[11] Both the MP2 and B3LYP methods reasonably reproduce the X-ray structures, while the HF method does not.[2a] The B3LYP method gives energetics similar to that obtained with the CCSD(T) method with much less cost.[2a] The calculations with the all-electron basis set afforded data comparable to those obtained with the relativistic-effective core potential such as Stuttgart[12] for the Cu atom. Stationary points were adequately characterized by normal-coordinate analysis.

Kinetic isotope effects were computed by Bigeleisen-Mayer's equation[13] with Wigner tunnel correction (eq 1) based on the calculated frequencies scaled by 0.945 at the B3LYP/321AS level. Here, $u$ donates $h\nu_i/kT$ and $\nu_i^{\ddagger}$ represents the frequency

$$k_L/k_H = \{(\nu_{1L}^{\ddagger}/\nu_{2L}^{\ddagger})\prod_i^{3n-7}[(u_{1i}^{\ddagger}/u_{2i}^{\ddagger})(e^{-u_{1i}^{\ddagger}/2}/e^{-u_{2i}^{\ddagger}/2})((1-e^{-u_{2i}^{\ddagger}/2})/(1-e^{-u_{1i}^{\ddagger}/2}))]\prod_i^{3n-6}[(u_{2i}^{\ddagger}/u_{1i}^{\ddagger})(e^{-u_{2i}^{\ddagger}/2}/e^{-u_{1i}^{\ddagger}/2})((1-e^{-u_{1i}})/(1-e^{-u_{2i}}))][1+(1/24)(h\nu_{1L}^{\ddagger}/kT)^2]\}\Big/[1+(1/24)(h\nu_{2L}^{\ddagger}/kT)^2] \quad (1)$$

in $cm^{-1}$, $T$ is the absolute temperature in K, $h$ is Planck's constant, and $k$ stands for the Boltzmann constant. A scale factor of 0.945 was derived from the product between the scale of 0.9614 for B3LYP/6-31G(d) frequencies[14] and the ratio of the B3LYP/631AS frequencies with the B3LYP/321AS frequencies for the transition state in the addition of $(Me_2CuLi)_2$ to acrolein.[2b] For NMR chemical shift calculations, we employed gauge including the atomic orbital (GIAO)-B3LYP method combined with the Ahlrichs-DZP all-electron basis set[9] for Cu and 6-311+G(d)[10] basis sets for the rest (denoted as B3LYP/6311AD). A basis set of at least triple-ζ quality and at least one set of polarization functions is needed to obtain reasonable NMR data but was found still not to be so accurate as one might desire.[1c] Natural charges were calculated by the natural population analysis[15] at the same level as that used for geometry optimization.

## Solvent Effects on Conjugate Addition to Acrolein

We first studied the solvated model of the reaction of $Me_2CuLi{\cdot}LiCl$ and acrolein (**Ia**) by coordination of up to two molecules of $Me_2O$ on each lithium atoms (**Ib**−**d**). The effects of solvent coordination on the lithium atoms were systematically examined for the structures and energetics (Figure 2 and Table 1). For such large calculations, we employed only the B3LYP/321AS level. We found that the structures of **Ia** and **TS·Ia** at the B3LYP/321AS and at the B3LYP/631AS level (first and second rows in Table 1) are almost the same as each other, except for the O−Li bond lengths, which are slightly shorter at the B3LYP/321AS level.

In all structures of the solvated models **Ib**−**d** as well as of **Ia** (Figure 1 and Table 1), $r^1$ (ca. 2.4−2.6 Å) and $r^2$ (ca. 2.1−2.2 Å) are longer than $r^3$ (ca. 2.0 Å). In addition,

(7) Ouannes, C.; Dressaire, G.; Langlois, Y. *Tetrahedron Lett.* **1977**, 815−818.

(8) Frisch, M. J.; Trucks, G. W.; Schlegel, H. B.; Scuseria, G. E.; Robb, M. A.; Cheeseman, J. R.; Zakrzewski, V. G.; Montgomery, J. A., Jr.; Stratmann, R. E.; Burant, J. C.; Dapprich, S.; Millam, J. M.; Daniels, A. D.; Kudin, K. N.; Strain, M. C.; Farkas, O.; Tomasi, J.; Barone, V.; Cossi, M.; Cammi, R.; Mennucci, B.; Pomelli, C.; Adamo, C.; Clifford, S.; Ochterski, J.; Petersson, G. A.; Ayala, P. Y.; Cui, Q.; Morokuma, K.; Malick, D. K.; Rabuck, A. D.; Raghavachari, K.; Foresman, J. B.; Cioslowski, J.; Ortiz, J. V.; Stefanov, B. B.; Liu, G.; Liashenko, A.; Piskorz, P.; Komaromi, I.; Gomperts, R.; Martin, R. L.; Fox, D. J.; Keith, T.; Al-Laham, M. A.; Peng, C. Y.; Nanayakkara, A.; Gonzalez, C.; Challacombe, M.; Gill, P. M. W.; Johnson, B. G.; Chen, W.; Wong, M. W.; Andres, J. L.; Head-Gordon, M.; Replogle, E. S.; Pople, J. A. *Gaussian 98*, revision A.6; Gaussian, Inc.: Pittsburgh, PA, 1998.

(9) Schafer, A.; Horn, H.; Ahlrichs, R. *J. Chem. Phys.* **1992**, *97*, 2571.

(10) Hehre, W. J.; Radom, L.; von Ragué Schleyer, P.; Pople, J. A. *Ab Initio Molecular Orbital Theory*; Wiley: New York, 1986, and references cited therein.

(11) See the previous article for the evaluation of computational methods: Yamanaka, M.; Inagaki, A.; Nakamura, E. preceding manuscript.

(12) Dolg, M.; Wedig, U.; Stoll, H.; Preuss, H. *J. Chem. Phys.* **1987**, *86*, 866−872.

(13) (a) Bigeleisen, J.; Mayer, M. G. *J. Chem. Phys.* **1947**, *15*, 261−267. (b) Bigeleisen, J.; Wolfsberg, M. *Adv. Chem. Phys.* **1958**, *1*, 15−76. (c) Yamataka, H.; Nagase, S. *J. Am. Chem. Soc.* **1998**, *120*, 7530−7536.

(14) Scott, A. P.; Radom, L. *J. Phys. Chem.* **1996**, *100*, 16502−16513.

(15) Reed, A. E.; Weinstock, R. B.; Weinhold, F. *J. Chem. Phys.* **1985**, *83*, 735−746.

**Table 1. Difference of the Structures (Å) and the Activation Energies ($\Delta E^{\ddagger}$) between Nonsolvated and Solvated Models of "$Me_2CuLi{\cdot}LiCl$ + Acrolein"**

| | $S^1$ | $S^2$ | $r^1$ (Å) | $r^2$ (Å) | $r^3$ (Å) | $r^4$ (Å) | $r^5$ (Å) | $r^6$ (Å) | $r^7$ (Å) | $\Delta E^{\ddagger}$ (kcal/mol)[a] |
|---|---|---|---|---|---|---|---|---|---|---|
| **Ia**[b] | none | none | 2.500 | 2.164 | 2.000 | 1.977 | 2.025 | 2.153 | | |
| **Ia** | none | none | 2.460 | 2.155 | 2.016 | 1.978 | 2.018 | 2.190 | | |
| **Ib** | $Me_2O$ | $Me_2O$ | 2.372 | 2.138 | 2.033 | 1.969 | 1.987 | 2.638 | | |
| **Ic** | $Me_2O$ | 2 $Me_2O$ | 2.404 | 2.134 | 2.027 | 1.971 | 1.989 | 2.687 | | |
| **Id** | 2 $Me_2O$ | 2 $Me_2O$ | 2.574 | 2.164 | 2.003 | 1.977 | 1.982 | 4.024 | | |
| **TS·Ia**[b] | none | none | 2.534 | 2.155 | 2.100 | 2.122 | 1.997 | 2.218 | 2.095 | 9.6 |
| **TS·Ia** | none | none | 2.526 | 2.147 | 2.108 | 2.124 | 1.997 | 2.247 | 2.105 | 9.1 |
| **TS·Ib** | $Me_2O$ | $Me_2O$ | 2.490 | 2.133 | 2.106 | 2.142 | 1.989 | 2.514 | 2.107 | 10.6 |
| **TS·Ic** | $Me_2O$ | 2 $Me_2O$ | 2.495 | 2.130 | 2.111 | 2.149 | 1.977 | 2.597 | 2.100 | 10.9 |
| **TS·Id** | 2 $Me_2O$ | 2 $Me_2O$ | 2.724 | 2.180 | 2.095 | 2.133 | 1.969 | 4.262 | 2.068 | 12.3 |

[a] $\Delta E^{\ddagger}$ refers to the energy difference between **I** and **TS·I**. [b] Geometry optimization was performed at the B3LYP/631AS level.

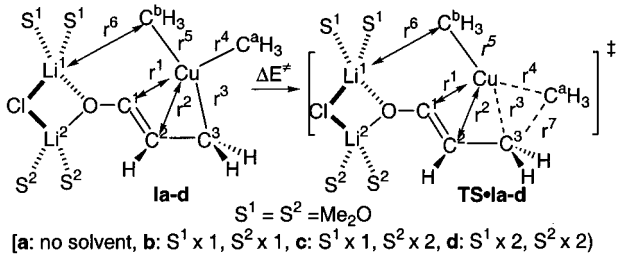


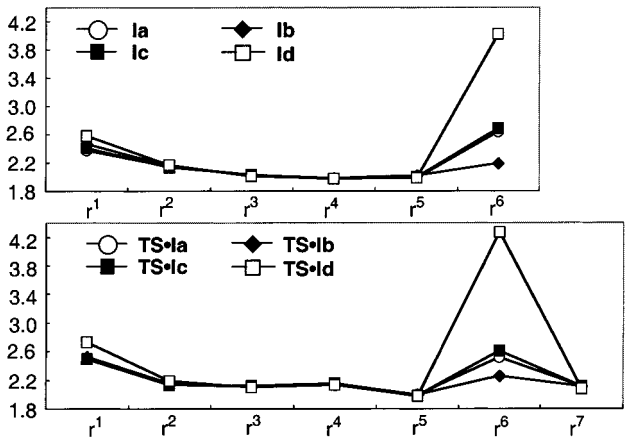


**Figure 2.** Comparison of the interatomic distances (Å) of nonsolvated and solvated models of "$Me_2CuLi{\cdot}LiCl$ + acrolein". All structures were optimized at the B3LYP/321AS level. $\Delta E^{\ddagger}$ refers to the energy difference between **I** and **TS·I**.

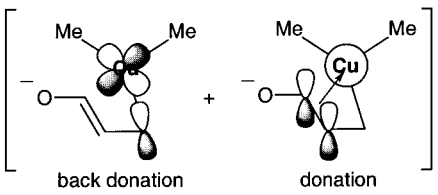


**Figure 3.** Schematic description of the cuprate/enone complex as a linear combination of two localized orbitals.[1a,2b]

the $C^3$ atom is pyramidalized (351.1−352.9°), while the $C^2$ atom is almost flat (358.2−359.2°), regardless of solvent coordination. This is consistent with the previous localized orbital analysis[1b] (Figure 3) that the Cu−$C^3$ bond is a $\sigma$-bond mainly due to the filled Cu $3d_{xz}$ orbital (i.e., back-donation), and the Cu−$C^2$ bond is due to $\pi$-coordination from the enolate to the vacant 4s orbital (donation; for further discussion, see Conclusion).

The $Li^1$−$C^bH_3$ distance ($r^6$) becomes longer as the number of $Me_2O$ coordination on the $Li^1$ atom increases.

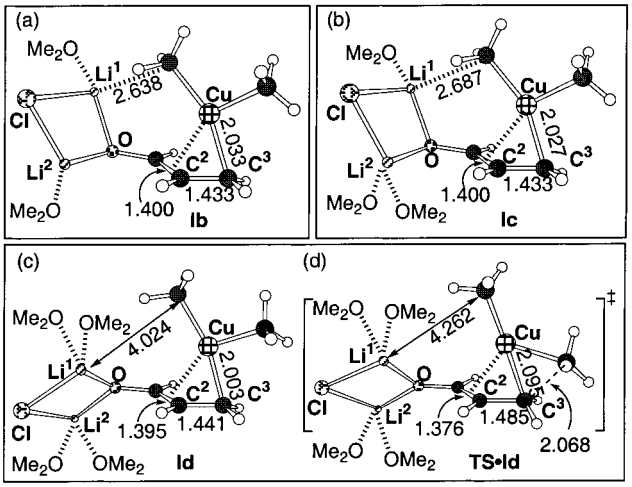


**Figure 4.** 3D structures of (a) **Ib**, (b) **Ic**, (c) **Id**, and (d) **TS·Id**. All structures were optimized at the B3LYP/321AS level. Distances are in Å.

The $Li^1$ atom in **Ib** and **Ic** is tetracoordinated (Figure 4a,b), and remains so when two molecules of $Me_2O$ are allowed to coordinate on the $Li^1$ atom in **Id** and **TS·Id**. In the latter, however, the $Li^1$−$C^bH_3$ coordination is replaced by $Li^1$−$OMe_2$ (Figure 4c,d). The structure around the Cu(III) center, on the other hand, remains virtually unaffected by solvent coordination on the lithium atoms (Figure 1). The degrees of pyramidalization of $C^2$ and $C^3$ atoms are not much affected by solvation either (vide supra).

The activation energy ($\Delta E^{\ddagger}$) shows strong correlation to the number of $Me_2O$ coordination on the lithium atoms (Table 1). As the number of the $Me_2O$ coordination increases, the activation energy becomes larger (**TS·Ia**, +9.6 kcal/mol; **TS·Ib**, +10.6 kcal/mol; **TS·Ic**, +10.9 kcal/mol; **TS·Id**, +12.3 kcal/mol). Thus, both the structural properties and the energetics of the Cu(III) complex are affected by the number of $Me_2O$ coordination. To examine the correlation of the structural change by solvent coordination to the energetics of the Cu(III) complex, we studied the charge distribution of both the nonsolvated (i.e., from **Ia** to **TS·Ia**) and the solvated (i.e., from **Id** to **TS·Id**) models (Figure 5). In both models, the positive charge on the Cu(III) center and the negative charge on the $C^aH_3$ and $C^3H_2$ groups, where the C−C bond formation occurs, decrease during the reductive elimination process. In contrast, the negative charge on the $C^bH_3$ group increases as the C−C bond forms. The charge distribution of Li, Cl, and carbonyl oxygen remains virtually constant throughout the reac-

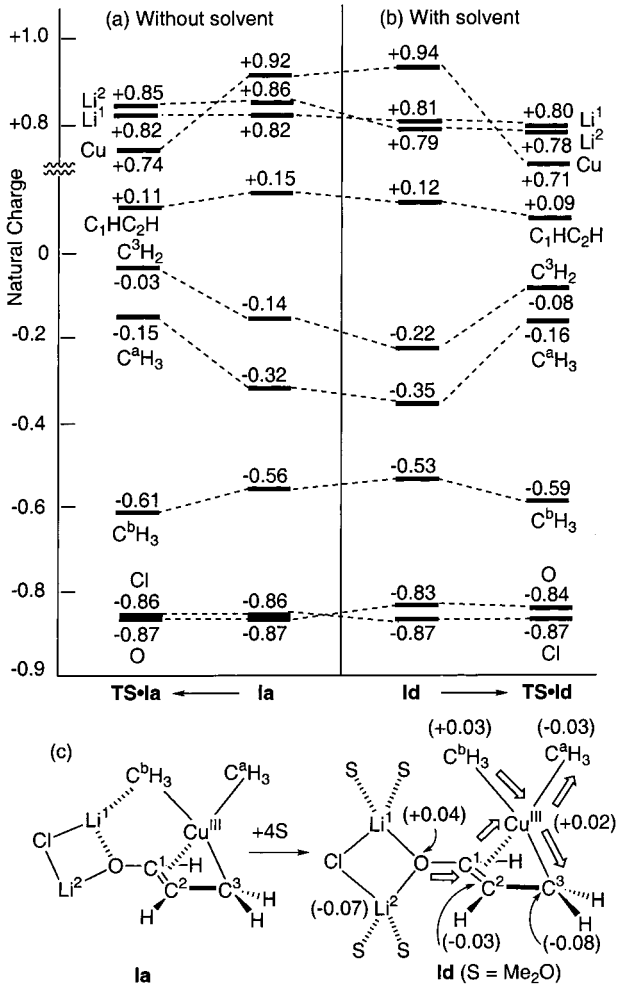


**Figure 5.** (a, b) Natural population analysis of the nonsolvated model (a, **Ia** and **TS·Ia**) and the solvated model (b, **Id** and **TS·Id**) at the B3LYP/321AS level. All structures are optimized at the same level. (c) Changes of the charge distribution upon going from **Ia** to **Id** (in parentheses) and arrows in **Id** showing the charge transfer by association of solvent from the lithium atoms.

tion, and the olefinic carbons (i.e., $C^1HC^2H$) are charged slightly positive due to the $\pi$-coordination to the Cu(III) center (cf. Figure 3).

The comparison of charge distributions between the nonsolvated (i.e., **Ia**) and the solvated models (i.e., **Id**) gave us a direct clue to understand the retardation of the $C^3-C^a$ bond formation upon solvation of the lithium atoms (Figure 5c). The charge on the core structure in the solvated model **Id**, excluding all $Me_2O$ molecules, is $-0.14$, which represents the total negative charge donated from the $Me_2O$ molecules. This excess negative charge in **Id** resides largely on $C^3$ ($-0.08$) and partly on $C^aH_3$ ($-0.03$). Such a buildup of negative charge on $C^3$ and $C^a$, which undergo C−C bond formation through a reductive elimination mechanism, inevitably increases the activation energy of this C−C bond-forming process.[16] The negative charge on $C^3$ and $C^a$ is increased, partly due to the increase of negative charge on the $C^2$ atom and partly due to the loss of coordination of the Lewis acidic $Li^1$ to $C^bH_3$ (cf. arrows). A solvent-separated ion pair (SSIP) is a less reactive species than a contact ion pair (CIP) (Scheme 1). This is because the Lewis acidity of the lithium atoms in an SSIP is eliminated, which retards the reductive elimination process.

(16) Nakamura, E.; Yamanaka, M.; Mori, S. *J. Am. Chem. Soc.* **2000**, *122*, 1826−1827.

**Table 2. (a) Details of the Cu(III) Intermediates and Transition Structures for IId and IIId around Cu(III) Center at the B3LYP/321AS Level and (b) the Natural Charge and Activation Energies (kcal.mol) at the B3LYP/321AS Level**

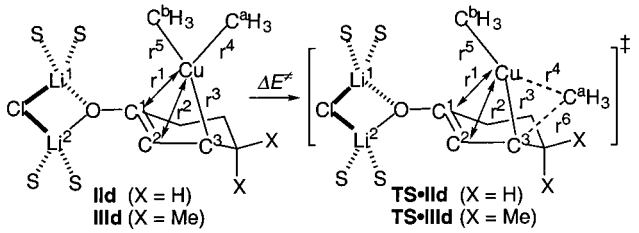


(a) Intermediates and Transition States

| | $r^1$ (Å) | $r^2$ (Å) | $r^3$ (Å) | $r^4$ (Å) | $r^5$ (Å) | $r^6$ (Å) | $\varphi^a$ (deg) | $\theta^b$ (deg) |
|---|---|---|---|---|---|---|---|---|
| **IId** | 2.769 | 2.147 | 2.007 | 1.980 | 1.989 | | 86.0 | 167.7 |
| **IIId** | 2.700 | 2.129 | 2.023 | 1.979 | 1.993 | | 83.0 | 160.8 |
| **TS·IId** | 2.802 | 2.162 | 2.120 | 2.124 | 1.971 | 2.094 | 90.3 | 162.8 |
| **TS·IIId** | 2.724 | 2.166 | 2.134 | 2.133 | 1.971 | 2.100 | 84.7 | 149.2 |

(b) Natural Charge and Activation Energies

| | $C^1$ | $C^2H$ | $C^3H$ | Cu | $C^aH_3$ | $\Delta E^{\ddagger}$ (kcal/mol) |
|---|---|---|---|---|---|---|
| **IId** | 0.41 | −0.25 | −0.20 | 0.93 | −0.37 | |
| **IIId** | 0.39 | −0.23 | −0.20 | 0.95 | −0.37 | |
| **TS·IId** | 0.39 | −0.26 | −0.07 | 0.72 | −0.17 | 12.4 |
| **TS·IIId** | 0.38 | −0.25 | −0.05 | 0.73 | −0.17 | 15.5 |

[a] $\varphi = \angle C^1-C^2-C^3-Cu$. [b] $\theta = \angle C^2-C^3-Cu-C^a$.

## Substituent Effects on Conjugate Addition to Cyclohexenone Derivatives

**(1) Activation Energy.** To probe the issue of the substituent and solvent effects on cuprate conjugate addition, the calculated activation energy was studied for the reaction of the dimethylcuprate and cyclohexane (**IId**) vs 4,4-dimethylcyclohexenone (**IIId**). For the latter, experimental data are now available.[6] Details of the Cu(III) complexes (**IId**, **IIId**) and the transition structures (**TS·IId**, **TS·IIId**) are shown in Table 2. The olefinic $C^1-C^2$ moiety internally coordinates on the Cu(III) center to form a near-square-planar structure around the Cu(III) center (cf. Figure 2). The very long $Li^1-C^bH_3$ distance is the major geometrical feature in the solvated model, as discussed in the previous section. The activation energy for **TS·IId** is 2.4 kcal/mol larger than that for the corresponding nonsolvated model of "$(Me_2CuLi)_2$ + cyclohexenone"[1b,c] ($\Delta E^{\ddagger} = 10.0$ kcal/mol). The increase is similar in magnitude to that found for the acrolein case discussed in the previous section.

Though **IIId** is very similar in structure to **IId**, **TS·IIId** differs from **TSIId** for the dihedral angle $\theta$, which is much smaller (162.8° in **TS·IId**, 149.2° in **TS·IIId**). This indicates that the $C^aH_3$ group in **TS·IIId** attacks the $C^3$ atom from the outside of the cyclohexene ring to avoid steric hindrance of the *gem*-dimethyl group. The steric hindrance of the *gem*-dimethyl group increases the activation energy by 3.1 kcal/mol. Thus, the 15.5 kcal/mol activation energy for the reaction of 4,4-dimethylcyclohexenone with $Me_2CuLi{\cdot}LiCl{\cdot}4Me_2O$ (B3LYP/321AS//B3LYP/321AS, B3LYP/631AS//B3LYP/

**Table 3. Experimental and Computational (B3LYP/321AS) KIE Values for the Nonsolvated Model of TS·IVa and TS·VIa[1c] and the Solvated Model of TS·IId and TS·Vd with the Bigeleisen−Mayer Equation, Including the Wigner Tunnel Effect**

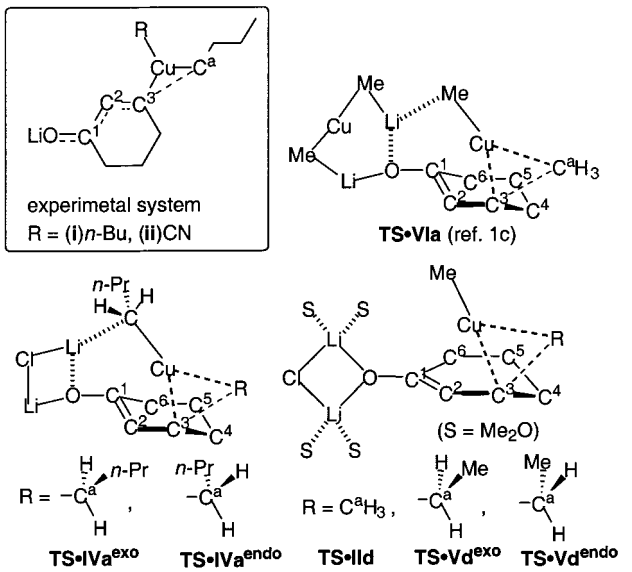


| | $C^1$ | $C^2$ | $C^3$ | $C^4$ | $C^5$ | $C^6$ | $C^a$ |
|---|---|---|---|---|---|---|---|
| expt i | 1.002 | 1.005 | 1.023 | 0.998 | 1.005 | 1.000 | 1.014 |
| expt ii | | | | | | | 1.020 |
| **TS·VIa** | 0.999 | 1.006 | 1.018 | 0.997 | 1.000 | 1.000 | 1.032 |
| **TS·IId** | 1.001 | 1.008 | 1.020 | 0.997 | 1.000 | 1.000 | 1.034 |
| **TS·IVA$^{exo}$** | 1.002 | 1.005 | 1.019 | 1.000 | 1.000 | 1.000 | 1.029 |
| **TS·IVa$^{endo}$** | 1.000 | 1.006 | 1.019 | 0.998 | 1.000 | 1.000 | 1.025 |
| **TS·Vd$^{exo}$** | 1.001 | 1.005 | 1.018 | 0.996 | 1.000 | 1.000 | 1.029 |
| **TS·Vd$^{endo}$** | 1.000 | 1.007 | 1.022 | 0.998 | 1.009 | 1.000 | 1.026 |

321AS; 15.2 kcal/mol)[17] is closer to the experimental data for the same enone and $Me_2CuLi{\cdot}LiI$ ($E_a = 18.2 \pm 1.7$ kcal/mol).[6] Natural population analysis showed that the charge distributions in both **IId** and **TS·IId** are very close to those of **IIId** and **TS·IIId**, respectively (Table 2b). Therefore, we conclude that the difference of the activation energies in the two series (3.1 kcal/mol) is not due to electronic effects but largely due to the steric hindrance of the *gem*-dimethyl group.

**(2) Kinetic Isotope Effect.** Experimental KIEs provide valuable information on the nature of the transition state. Recent experimental studies on the conjugate addition of $Bu_2CuLi{\cdot}LiBr{\cdot}SMe_2$ (**i**) revealed a sizable KIE on the two carbon atoms associated with the $\sigma$-bond formation, $C^3$ (1.023) and $C^a$ (1.014)[18] (Table 3). Other carbon atoms on the enone showed very small KIE values indicative of small changes of bonding state in the transition state. Note that KIEs of Bu(CN)CuLi (**ii**) showed a much larger $C^a$ value (1.020) than for $Bu_2CuLi{\cdot}LiBr{\cdot}SMe_2$ (**i**) (1.014). This indicates the presence of considerable substituent effects on cuprate KIE, but the reason has thus far remained unclear. To study what factors may affect the KIE in the cuprate reactions, a nonsolvated model of "$Bu_2CuLi{\cdot}LiCl$ + cyclohexenone" (**TS·IVa**), solvated models of "$Me_2CuLi{\cdot}LiCl$ + cyclohexenone" (**TS·IId**) and "Me(Et)CuLi·LiCl + cyclohexenone" (**TS·Vd**) were compared. For **TS·IVa** and **TS·Vd**, two conformational isomers (i.e., exo and endo) with regard to the nucleophilic carbon center (i.e., $C^a$) were also studied.[19] With its large size and numerous conformational possibilities, the solvated model of "$Bu_2CuLi{\cdot}LiCl$ + cyclohexenone" was not studied.

The two carbon atoms associated with the C−C bond formation, $C^3$ and $C^a$, showed large KIE values in all chemical models (Table 3). All chemical models give the KIE values of $C^1$−$C^5$ close to the experimental value (the deviation being less than −0.5%).[20] In contrast, the KIE values of $C^a$ depend very much on the chemical models. The KIE of the nonsolvated $(Me_2CuLi)_2$ model **TS·VIa** and the solvated $Me_2CuLi{\cdot}LiCl$ model **TS·IId** are very similar to each other and show large KIE values on $C^a$ (1.032 and 1.034). The nonsolvated $Bu_2CuLi{\cdot}LiCl$ models **TS·IVa$^{exo}$** and **TS·IVa$^{endo}$**, however, showed much smaller $C^a$ KIE values[21] (1.029 and 1.025, respectively). The solvated Me(Et)CuLi·LiCl models **TS·V$^{exo}$** and **TS·V$^{endo}$** also showed smaller $C^a$ KIE values (1.029 and 1.026), respectively. Thus, the $C^a$ substituents of organocuprates exert some influence on the computation of $^{12/13}C$ KIEs.

To examine the factors that affect the $C^a$ KIE in **TS·IVa$^{endo}$** and **TS·IId**, the vibration modes that are most responsible for the observed $^{12/13}C$ KIEs were identified.[22] Four of these important vibration modes are shown in Figure 6. In both chemical models, the vibration modes $\nu_{CaC3}{}^{\ddagger}$ (Figure 6a,e) with the imaginary frequencies correspond to the C−C bond formation, which should be expected. The $C^a$−Cu stretching vibration modes (Figure 6b,c,f,g) correspond to the frequencies $\nu_{CaCu}$ in both chemical models. Note that the deformation vibration mode $\delta_{CH3}$ in **TS·IId** (Figure 6h) corresponds to the $C^a$−C stretching vibration $\nu_{CaC}$ in **TS·IVa$^{endo}$** (Figure 6d), since the center of gravity of the incoming group is the *n*-propyl group in the latter. This vibration mode therefore contributes most to the difference between $Me_2CuLi{\cdot}LiCl$ and $Bu_2CuLi{\cdot}LiCl$. We found little influence of the solvation on the vibration mode associated with the Li−Cl−Li moiety. This is because of the lack of structural change during the reductive elimination and explains why there are relatively small effects of solvent coordination on the computation of the $^{13}C$ KIEs of cuprate conjugate addition. Therefore, careful studies on the vibration modes of the incoming group (including the analysis of various conformers) are necessary for accurate computation of the $^{13}C$ KIEs in structurally complex reactions.

**(3) $^{13}C$ NMR Chemical Shift.** Experimental NMR measurements of intermediates of conjugate addition provided valuable reference points for probing the nature of intermediates in the reaction pathway. Unreactive enones bearing sterically hindered groups on

(17) Because of computational limitations, we could not examine the effect of bulk solvent on solvated models (SCRF calculation). We found, however, for nonsolvated models that the polarity has an effect of less than a few kcal/mol.[2]

(18) Frantz, D. E. Singleton, D. A.; Snyder, J. P. *J. Am. Chem. Soc.* **1997**, *119*, 3383−3384.

(19) The endo series of isomeric transition states stands at the slightly higher energy level than the exo series at the B3LYP/321AS level.

(20) The $C^6$ atom was used as an internal standard, assuming that its isotopic composition is not subject to KIE.

(21) The calculations of $^{12/13}C$ KIEs for the exo and endo series of **TS·IVa** and **TS·Vd** are based on the exo series of the Cu(III) complex, which must be in mobile equilibrium with the endo series.

(22) The ratio of $\nu_{^{12}C}/\nu_{^{13}C}$, which mainly determines the KIEs, is larger than other vibration modes, as shown in Bigeleisen−Mayer's equation.[9]

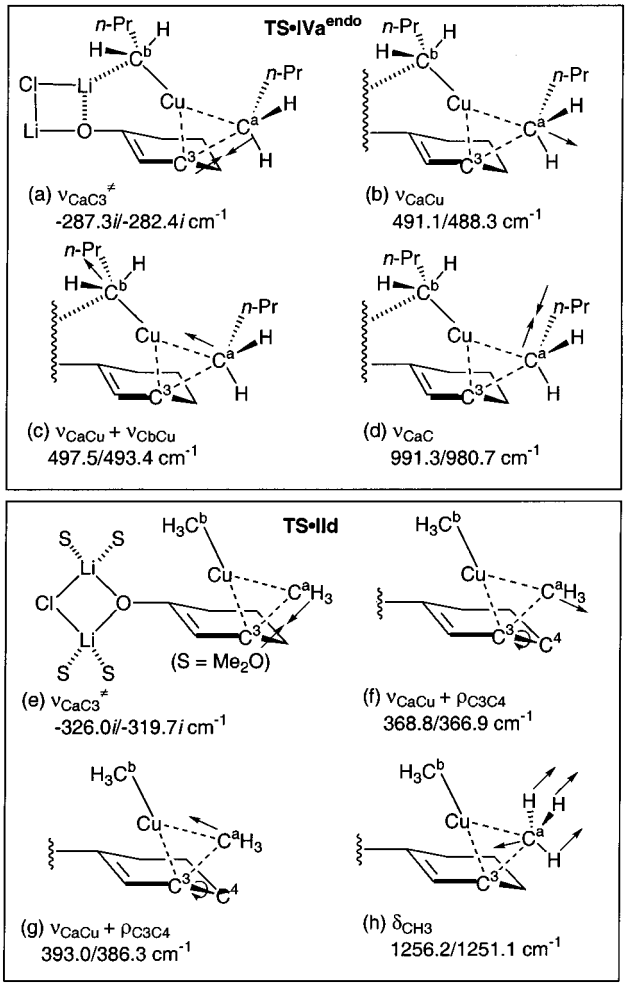


**Figure 6.** Schematic fundamental vibration modes for KIEs of $C^a$ in (a−d) **TS·IVa$^{endo}$** and (e−h) **TS·IId**. The frequencies for $^{12}C/^{13}C$ are shown.

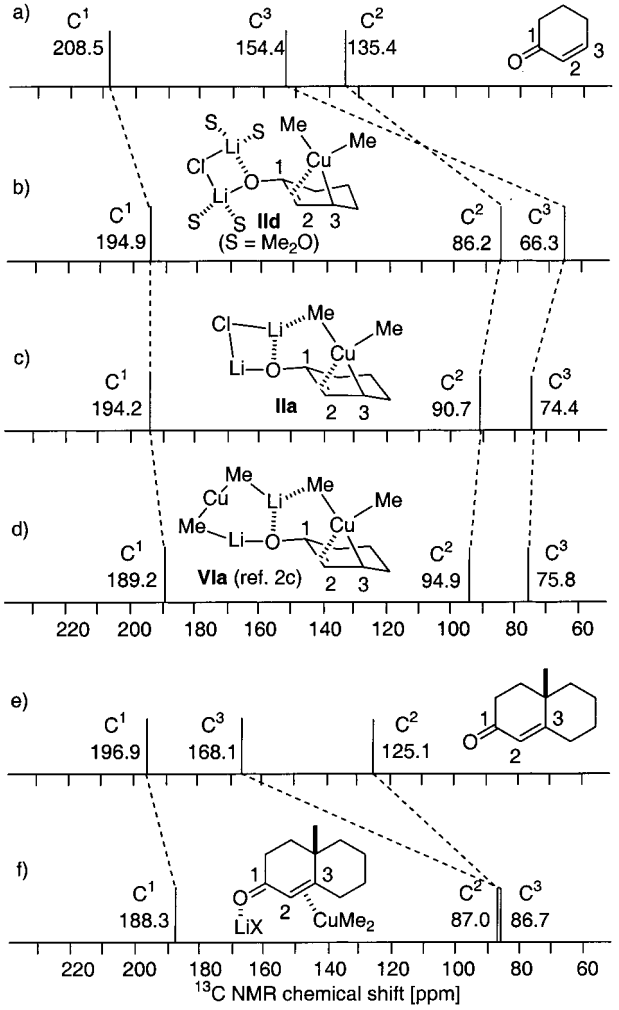


**Figure 7.** Calculated $^{13}C$ NMR chemical shifts for (a) 2-cyclohexenone, (b) solvated $\pi$ complex with $Me_2CuLi$·LiCl, (c) nonsolvated $\pi$ complex with $Me_2CuLi$·LiCl, and (d) nonsolvated $\pi$ complex with $(Me_2CuLi)_2$ and experimental $^{13}C$ NMR chemical shifts for (e) 10-methyl-$\Delta^{1,9}$−2-octalone and (f) its $\pi$ complex with $(Me_2CuLi)_2$ in diethyl ether-$d_{10}$.

the olefinic carbons are usually employed for the experimental NMR measurements.[23] However, computation of the $^{13}C$ NMR chemical shift, in which a basis set of at least triple-$\zeta$ quality and at least one set of polarization function is generally needed,[24] can only be performed for the simple model (i.e., acrolein, cyclohexenone) due to current computational limitation. The solvent effect for the $^{13}C$ NMR chemical shift was therefore studied at the B3LYP/6311AD//B3LYP/321AS level (Figure 7). The solvated model **IId** (Figure 7b) and a nonsolvated model **IIa** (Figure 7c) show similar tendencies of the carbonyl carbon to undergo a small upfield shift and the olefinic carbon to undergo a large upfield shift. These calculated $^{13}C$ NMR chemical shift values qualitatively agree with the related experimental data (Figure 7f).[1c] The small upfield shift (4−8 ppm) of the olefinic carbon upon going from **IIa** to **IId** is likely due to the increase of the negative charges on $C^2$ and $C^3$ because of the attenuation of the Lewis acidity of the Li atoms. The lithium bridge moiety (Cl or $Me_2Cu$) does not much affect the $^{13}C$ NMR chemical shift values (Figure 7c,d).[25] In summary, the salient features of the $^{13}C$ NMR chemical shift values of the intermediate can be reproduced with reasonable accuracy even without consideration of solvent coordination.

## Conclusion

Conjugate addition of an organocuprate to an $\alpha,\beta$-unsaturated ketone belongs to a class of transition metal/olefin reactions. One can draw a pair of donation and back-donation schemes for $Me_2Cu^-$ (nucleophile) and ethylene (electrophile) as in Figure 8a. This reaction, however, does not take place experimentally because ethylene is not electrophilic enough to accept electrons from the cuprate (i.e., insufficient back-donation: in contrast, acetylene composed of intrinsically

(23) (a) Bertz, S. H.; Smith, R. A. J. *J. Am. Chem. Soc.* **1989**, *111*, 8276−8277. (b) Hallnemo, G.; Olsson, T.; Ullenius, C. *J. Organomet. Chem.* **1984**, *265*, C22−C24. (c) Hallnemo, G.; Olsson, T.; Ullenius, C. *J. Organomet. Chem.* **1985**, *282*, 133−144. (d) Ullenius, C.; Christenson, B. *Pure Appl. Chem.* **1988**, 57−64. (e) Vellekoop, A. S.; Smith, R. A. J. *J. Am. Chem. Soc.* **1994**, *116*, 2902−2913. (f) Krause, N.; Wagner, R.; Gerold, A. *J. Am. Chem. Soc.* **1994**, *116*, 381−382.

(24) Helgaker, T.; Jaszunski, M.; Ruud. K. *Chem. Rev.* **1999**, *99*, 293−352.

(25) The $^{13}C$ NMR chemical shift values on $C^2$ and $C^3$ are considerably downfield shifted ($C^2$, 127.6 ppm; $C^3$, 107.4 ppm) by using the STO-3G basis set on the Cl atom. This indicates that the basis set effect is quite large for the calculation on the $^{13}C$ NMR chemical shift.[21]

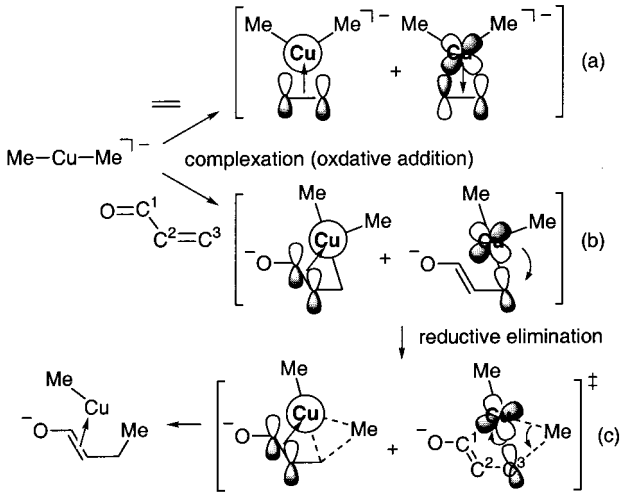


**Figure 8.** Localized orbital schemes responsible for bonding in (a) the cuprate/alkene complex, (b) the cuprate/enone complex, and (c) its transition state of the reductive elimination.[1a,2a,b]

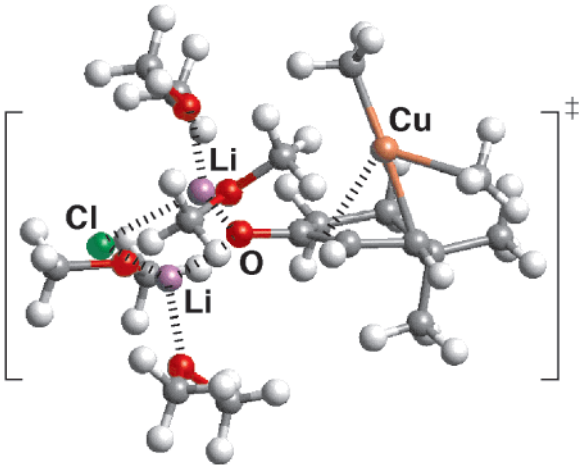


**Figure 9.** The 3D TS of the reaction between 4,4-dimethylcyclohex-2-en-1-one and $Me_2CuLi{\cdot}LiCl$ solvated with four molecules of dimethyl ether (**TS·IIId**). Color code: gray, carbon; white, hydrogen; red, oxygen; green, chlorine; orange, copper; purple, lithium.

electron-deficient sp carbon atoms is reactive toward organocuprate).[2a] Therefore, when ethylene is substituted with a carbonyl function (e.g., acrolein), it becomes electrophilic enough to react with $Me_2Cu^-$. The donation/back-donation scheme is now unsymmetrical, as shown in Figure 8b.[2b] The complex can be viewed as a T-shaped Cu(III) complex bearing an enolate donor as the fourth ligand in a square-planar coordination sphere. For the reductive elimination process in Figure 8c to take place, the Cu(III) center needs to recover electrons specifically from the $Cu-C^3$ atom, since the two electrons localized in this bond (Figure 8b) have largely originated from the copper atom. In other words, reductive elimination does not take place on the $C^1$ end because the electrons in the $C^1-Cu$ bond have largely originated from the carbon 2p orbital.

The effects of solvation of lithium atoms discussed in this article can be rationalized in the framework of the above analysis. Thus, the solvent coordination attenuates the Lewis acidity of the lithium atoms which are attached to the carbonyl oxygen. One consequence is the increase of the electron density on the $C^3$ atom, which increases the activation energy of the reductive elimination process. Another consequence is the loss of the $Li^1-C^aH_3$ coordination, which retards reductive elimination of the Cu(III) intermediate.[16] When one considers a solvent much more basic and polar (e.g., crown ether, HMPA) than the simple ethereal solvents considered here, they will totally kill the Lewis acidity of the lithium atoms and therefore shut off the reaction (as reported experimentally for crown ether solvation).[7]

Substituent effects were found to be quite large. Thus, the 4,4-*gem*-dimethyl group in 2-cyclohexenone exerts considerable steric hindrance (worth 3.1 kcal/mol), and the present model gives an activation energy (15.5 kcal/mol) quite close to the experimental value (18.2 ± 1.7 kcal/mol). The experimental and theoretical $^{12/13}C$ KIEs are quite close to each other. KIE values, however, were found to be susceptible to substituent effects and still need further studies to achieve exact matching between experiments and theory. NMR chemical shift studies indicated that computational chemical shift values reasonably reproduce the experiments. Overall, the present theoretical models have been found to exhibit good agreement with the experiments and will be useful for analysis and designing of organocuprate reactions.[26]

Finally, the organocopper chemistry that has a history of 70 years now may be regarded as an important subdivision of supramolecular chemistry—a concept created much more recently. The meaning of this statement may become immediately apparent if one takes a look at the remarkable degree of molecular assembly created in the reaction between 4,4-dimethylcyclohex-2-en-1-one and $Me_2CuLi{\cdot}LiCl$ solvated with four molecules of dimethyl ether (**TS·IIId**, Figure 9).

**Acknowledgment.** E.N. thanks Monbu Kagakusho (Grant-in-Aid for Scientific Research, Specially Promoted Research) for financial support of this project. Generous allotment of computational time from the Institute for Molecular Science, Okazaki, Japan, and the Intelligent Modeling Laboratory, The University of Tokyo, is gratefully acknowledged. M.Y. thanks the JSPS for a predoctoral fellowship.

**Supporting Information Available:** Tables giving geometries of the representative stationary points. This material is available free of charge via the Internet at http://pubs.acs.org.

OM0105270

(26) 3D structures and coordinates are available at: http://www.chem.s.u-tokyo.ac.jp/~common/Theo/Solv/title.